View

Recent Progress in Metal Oxide Based Materials as Anode Materials for Lithium-Ion Batteries

Lili Feng[1,2,*], Changwei Su[1,2], Zhewen Xuan[1,2], Junming Guo[1,2], Yingjie Zhang[1,2]

[1] Engineering Research Center of Biopolymer Functional Materials of Yunnan, Yunnan University of Nationalities
[2] Key Laboratory of Ethnic Medicine Resource Chemistry, State Ethnic Affairs Commission & Ministry of Education, School of Chemistry and Biotechnology, Yunnan University of Nationalities, Kunming, China 650500

* Corresponding author: lilylian2003@163.com

Abstract

Transition metal oxides are promising anode materials for Li-ion batteries due to their high theoretical capacity (> 600 mAhg^{-1}), good rate capability, good safety, environmental friendliness and relatively low cost. In recent years, more and more investigators are motivating this advanced material rapidly towards their hybrid materials preparation to improve the cycling performance. Herein, we outlined the current research advances of transition metal oxides and their hybrid materials as anode materials for Li-ion batteries in the synthesis, lithium storage mechanism and electrochemical performance, with the aim of stimulating more research to achieve more useful application as soon as possible.

Keywords: Lithium-ion battery; Anode materials; Transition metal oxides; Electrochemical performance

1. Introduction

In recent years, as the development of the economy, the requirement and consumption of energy is increasing. New green high-performance secondary power as a clean and efficient energy storage and conversion device, plays an important role in new energy exploitation and environmental protection, and has become one of the areas of worldwide competing for the development. Lithium-ion battery is widely used in mobile electronic devices, electric vehicles, alternate energy storage, smart electricity grid system and other fields [1], due to its high voltage, high energy, light weight, small size, low internal resistance, low self-discharge, long cycle life, no memory effect [2,3]. With the application range continuously extends, it requires significant improvements in many perspectives of lithium-ion battery, such as higher nergy density, larger power density, longer cycle life, safety and lower cost. The key to the success of development of novel and advanced rechargeable lithium-ion battery is the improvement of electrode materials.

Much effort had been devoted to improve the performance of LIBs up to now, among which a lot of research work focused on finding alternative anode materials. Currently, the commercial LIBs anode material was graphite, coke and non-graphitized carbon [4-6]. However,

the theoretical capacity of graphite (372 mAhg^{-1}) could not be able to meet the needs of a new generation of high specific capacity LIBs. Now, the research focus of anode material for LIBs was mainly on the tin-based [7-9], silicon-based [10,11], antimony-based materials and the transition metal oxide materials [12-14]. Tin, silicon, and antimony-based anode materials were some of the most promising anode materials in view of the large theoretical capacity, rapid charge-discharge capacity, and easy to process, etc.. For examples, the theoretical specific capacity of tin-based materials was about twice larger than that of graphite's [15], and it was up to 4200 mAhg^{-1} of the silicon-based material. However, the following defects restricted the commercial application: 1. large volume change during charge and discharge process; 2. difficult to obtain good electrochemical performance when worked at high current density; 3. high initial irreversible capacity loss. Therefore, new anode materials were desired. Intensive efforts had been devoted to explore new anode materials or design novel nanostructures. As early as 2000, Tarascon's research group reported that electrodes made of nanoparticles of transition-metal oxides (MO, where M is Co, Ni, Cu or Fe) demonstrated electrochemical capacities of 700mAh

g⁻¹ (this value was approximately twice of the theoretical capacity of the carbon material [12]), with 100% capacity retention for up to 100 cycles and high recharging rates for the first time. Up to now, the anode material research was mainly on various transition metal oxides and their composite materials, shuch as Fe_3O_4, Co_3O_4, MnO_2, SnO_2, CuO, MoO_2, NiO, and V_2O_5. Chen group [15] reported α-Fe_2O_3 nanotubes were synthesized by templating method and studied as LIBs anode materials. It was found that the as-prepared α-Fe_2O_3 nanotubes, characterized by uniform size and shape with a high specific surface area, exhibited superior electrochemical activity, with a discharge capacity of 1415 mAhg⁻¹ at 100 mAg⁻¹ and 20 °C. Xie group [16] prepared SnO_2 hollow sphere and rod materials by the oxidation-crystallization method of amorphous colloids. The measured capacities of SnO_2 hollow sphere and rod electrodes were 698 and 470 mAhg⁻¹, respectively. And they were higher than that of a solid SnO_2 nanoparticles electrode (650 mAhg⁻¹). Hu et al [17] prepared the 3D hollow dendritic shaped CuO materials, and the average coulombic efficiency was up to 97.0% in 50 week cycle when discharged at 0.5C. Therefore, many attempts to obtain variety of transition metal oxides and their composite materials with excellent electrochemical performance had been carried out.

Herein, we outlined the current research advances of transition metal oxide materials as anode materials for LIBs in lithium storage mechanism, transition metal oxide nanomaterial preparation, hollow structure and core-shell structure construction of transition metal oxide materials, with an aim of stimulating more research to construct new metal oxide anode materials with high specific capacity, cycling performance, high coulombic efficiency, good rate capability and good safety, and achieve practical application as soon as possible.

2. Lithium storage mechanism and the defect of transition metal oxide materials

Up to now, there were three categories of LIBs anode materials, such as graphite, tin, silicon, antimony-based materials and the transition metal oxide materials. The lithium storage mechanisms of the three of the material types were different from each other. Graphite, a layered intercalation compound, was one of the most widely used lithium anodes. Lithium could be reversible inserted and extracted into the layered structure during the discharge/ charge process. The lithiated compounds had stable phases up to the LiC_6 stoichiometry corresponding to a theoretical specific capacity of 372 mAhg⁻¹. Tin, silicon, antimony-based materials had specific capacity much higher than the conventional graphite.

The lithium storage mechanism of the tin, silicon, antimony-based materials were based on the alloying and dealloying of Li and Sn, Si, or Sb in the discharge/charge process. The detailed reaction was as follows:

$$Si(Sn) + Li^+ + xe^- \rightleftharpoons Li_xSi(Sn), \quad X_{max}=4.4$$
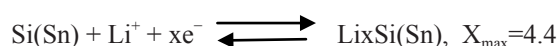
Although, both the lithium storage mechanism of the two materials were the same, Si was much more appealing for the relatively high content on the earth, and larger theoretical specific capacity which up to 4198 mAhg⁻¹ (about four times of the Sn electrode, 11 times of the graphite electrode). Unfortunately, there were 300% volume expansion during the alloying process of Li and Sn or Si, which suggested the destruction of the material integrity due to the enormous mechanical stress and pulverizes even if good reversibility during the charge/ discharge cycles.

Besides the intercalation compounds and metal alloys, another category of anodes were based on a conversion reaction, such as transition-metal oxides (MO, where M is Co, Ni, Cu or Fe and so on). The mechanism of Li reactivity differed from the classical Li insertion/ deinsertion or Li-alloying process, and involved the formation and decomposition of Li_2O, accompanying the reduction and oxidation of metal nanoparticles respectively. The detailed reaction was as follows:

$$M_xO_y + 2yLi \rightleftharpoons yLi_2O + xM$$
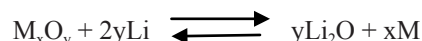
The formation of Li_2O and M was thermodynamically feasible. During the initial discharge process, M_xO_y nanoparticles were fully reduced by Li, which led to the formation of metallic M with nanosize and Li_2O nanoparticles. The generating metallic M was of high activity and dispersed in a lithia (Li_2O) matrix, with the (Li_2O nanoparticles) being surrounded by a solid electrolyte interface. The following charge process was inverse. The metallic M produced in the discharge process reacted with Li_2O, leading to the formation of nano transition metal oxides M_xO_y and Li. Indeed, Li_2O had always been reported to be electrochemically inactive, especially when reacted with tin, silicon, antimony-based materials. However, in this case, the electrochemically driven size confinement of the metal particles was thus believed to enhance their electrochemical activity towards the formation/decomposition of Li_2O. So, the cycling performances of the transition metal oxides materials as anode materials depended extremely on their degree of division or aggregation.

The theoretical specific capacities of the transition metal oxides materials could be calculated by:

$$C=(F*n)/(Mw*3.6)$$

Where F was Faraday's constant (96500 C mol⁻¹, 3.6 C = 1 mAh), n was the Li molar number which could be inserted into or react with the active material for per mole of active material, and Mw was the molar mass of the active material (g mol⁻¹). According to the formula, many theoretical specific capacities of transition metal oxides could be calculated. For example, the theoretical specific capacity of NiO was 718 mAhg⁻¹, Fe_3O_4 was 924 mAhg⁻¹, Fe_2O_3 was 1007 mAhg⁻¹, MnO_2 was 1232 mAhg⁻¹, CuO was 670 mAhg⁻¹, CoO was 715 mAhg⁻¹. The transition metal oxides exhibited large rechargeable capacities

58

Nano Biomed. Eng. 2013, 5(1), 57-64

which unrelated on the charge/discharge current and were much higher than that of the graphite (372 mAhg^{-1}). In addition, transition metal oxides materials had the advantages such as easy preparetion, low cost, high security, and similar redox potential to Li$^+$/Li. Therefore, transition metal oxides materials would act as promising candidates for electrode materials of LIBs.

Although transition metal oxides materials had large theoretical specific capacities, all these materials were generally plagued by large capacity loss during the initial cycle and poor cycling stability. There were two reasons for the large capacity loss during the initial cycle. (1) Transition metal oxides materials reacted with electrolyte resulting in the formation of a solid electrolyte interface (SEI) layer and possibly interfacial Li$^+$ storage. SEI film was known as a gel-like layer which contained ethylene oxide based oligomers, LiF, Li$_2$CO$_3$, and lithium alkyl carbonate (ROCO$_2$Li). The incompletely decomposition of SEI was the main reason for the large capacity loss during the initial cycle, which happened in all 3d transition metal oxides. So the lithium storage capacities were usually higher than the theoretical capacity. (2) After the first discharge, the resulting transition metal M and Li$_2$O could not be completely converted into M$_x$O$_y$ in the charge process.

There were three reasons for the poor cycling stability. (1) The electronic conductivity of transition metal oxides materials were usually low, and the electron or ion had difficults in the diffusion process, which resulting in irreversible electrode reaction and fast capacity decay. (2) After charge/discharge cycles, transition metal oxides suffered from enormous mechanical stress and pulverizes, leading to electrical contact loss between active particles and current collector. The transition metal oxides particles without electrical contact could no longer participate in the charge/discharge cycles, resulting in capacity fading. (3) The structural instability caused by gradual agglomeration of the metal grains, and the large volume change during phase transformation in the conversion reaction led to the capacity loss.

One effective way to mitigate these problems was to reduce the particle size of transition metal oxides to the nanometer scale. It was believed that the small particle size might short the diffusion length of the lithium ions, introduce ample contact area to the electrolyte as well as more active sites for lithium storage. Therefore, this article provided a simple overview on the nanostructured transition metal oxides materials and their hybrid materials as anode materials for LIBs.

3. The preparation of transition metal oxide materials and their electrochemical performance

The transition metal oxides as LIBs anode materials usually included SnO$_2$, CoO, NiO, CuO, Cu$_2$O, Fe$_2$O$_3$, Fe$_3$O$_4$, MnO$_2$ and so on. Among these transition metal oxides, SnO$_2$ was the most widely investigated because of their large capacity, environmental acceptability and low cost. The lithium storage mechanism was a little different as the traditional metal oxides for its two-step lithium storage. In the first process, SnO$_2$ was reduced to metallic Sn. The second process was the Sn alloying/de-alloying reaction with lithium. The overall electrochemical processes could lead to a total of 8.4 Li-ions insertion per formula unit of SnO$_2$. This corresponded to a theoretical capacity of 1491 mAhg^{-1}. H.K. Liu et al [18] reported on the preparation of SnO$_2$ nanowires by thermal evaporation process. The high purity SnO and Sn powders were mixed and mechanical milling for 40 h under an atmosphere of argon. Then, the ball-milled powder was placed in an alumina boat located inside a tube furnace, and silicon substrates without metal catalysts were placed downstream at a distance of about 15 cm from the powder to deposit SnO$_2$ nanowires. The SnO$_2$ nanowires showed initial capacity of 1134 mAhg^{-1}, and the capacity reduced to 250 mAhg^{-1} at the 50th cycle. In this report, traditional SnO$_2$ power was used as contrast. The initial capacity of the traditional SnO$_2$ power was about 580 mAhg^{-1}, and the capacity reduced to 100 mAhg^{-1} at the 50th cycle.
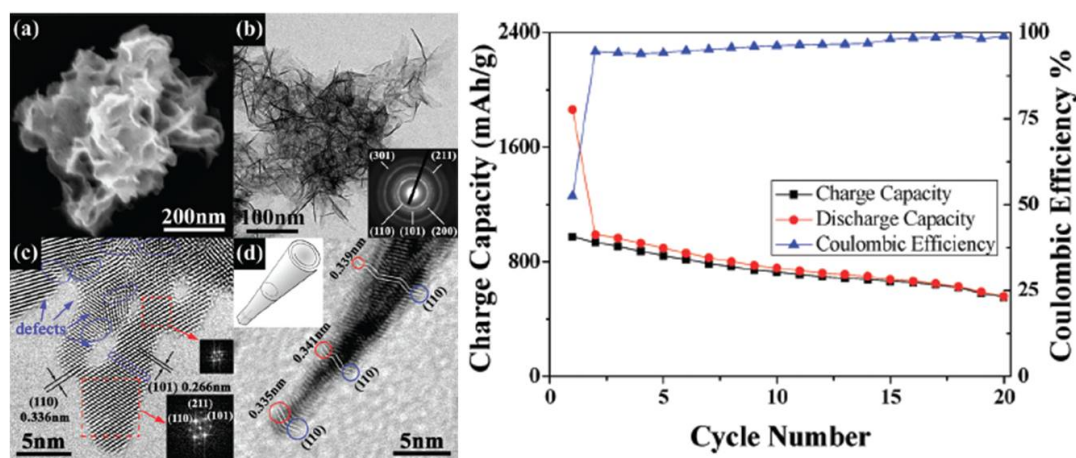

Figure 1 SEM image, TEM image, SAED pattern, and HRTEM images of the as-prepared SnO$_2$ nanosheets (left). Charge and discharge capacities as well as Coulombic efficiency as a function of cycle number with SnO$_2$ electrode in button cell (right). Reprinted with permission from C. Wang, Y. Zhou, M.Y. Ge, X.B. Xu, Z.L. Zhang, J.Z. Jiang, J. Am. Chem. Soc. 2010, 132, 46–47 by ACS publication.
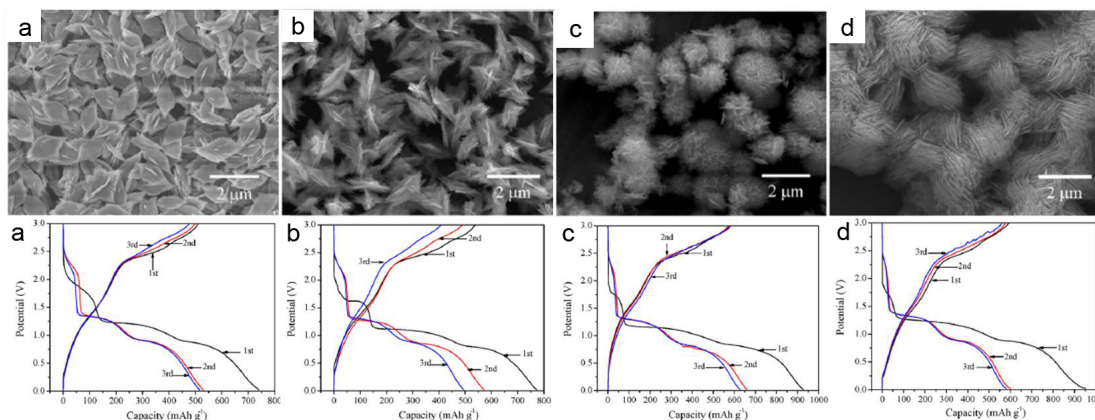
Figure 2 SEM images and the discharge-charge curves of CuO particles obtained under different pH conditions: (a) pH 9.5; (b) pH 10; (c) pH 11 and (d) pH 11.5. Reprinted with permission from J.Y. Xiang, J.P. Tu, L. Zhang, Y. Zhou, X.L.Wang, S.J. Shi, J. Power Sources, 2010, 195, 313–319 by Elsevier publication.

The improvement of electrochemical behavior could be attributed to the 1D nanowire structure with a large surface area and high length/diameter ratio. The smaller diameter of the nanowires provided a short diffusion length for Li$^+$ insertion, which could enhance the charge transfer and electron conduction along the length direction. J.Z. Jiang et al [19] reported highly porous SnO$_2$ nanometer-sized sheets synthesized from a hydrothermal reaction (the morphology and electrochemical cycle performance of the SnO$_2$ nanosheets were shown in Figure 1). The morphology of the assembled nanosheets revealed a three-dimensional, flower-like appearance. The SnO$_2$ nanosheets exhibited a high discharge capacity of 559 mAhg^{-1} after 20 cycles with the retention of 57%.

CuO was another promising material as LIBs anode materials as for its advantages of high theoretic capacity, inexpensive, non-toxic, easily produced, and readily stored. J.Y. Xiang et al [20] had synthesized hierarchical CuO particles with various morphologies such as leaf, shuttle, flower, dandelion, and caddice clew by dehydration and re-crystallization of precursor Cu(OH)$_2$ (shown in Figure 2). The initial capacity were 740 mAhg^{-1}, 773 mAhg^{-1}, 841 mAhg^{-1}, 927 mAhg^{-1}, 952 mAhg^{-1} respectively, and the initial coulombic efficiencies were 69.1%, 69.5%, 71.1%, 62.1% and 62.5%. The low coulombic efficiency and large capacity loss during the initial cycle could be attribute to the incompletely decomposition of SEI film. In the subsequent charge/discharge cycles, the charge capacity was 400 mAhg^{-1}. Compared to the theoretical capacity, the reversible capacity was not ideal. Tarascon research group [21,22] pointed out that Li$^+$ reacted with CuO in the discharge process, resulting elemental copper. But in the charge process, elemental copper could not be oxidized to the divalent state, and was usually oxidized to a monovalent state. Thus, the CuO samples had about 50% capacity loss.

B. V. R. Chowdari et al [23] prepared nanoflakes α-Fe$_2$O$_3$ on Cu foil by using radio frequency magnetron sputtering method. The morphology of the as-prepared α-Fe$_2$O$_3$ nanoflakes was shown in Figure 3. The samples exhibited a stable capacity of (680 ± 20) mAhg^{-1} with no

noticeable capacity fading up to 80 cycles when cycled in the voltage range 0.005-3.0 V at 65 mAg^{-1} (0.1 C rate). The capacity fading from the initial 1200 mAhg-1 to 680 mAhg^{-1} regarded to its detailed lithium storage mechanism. After the α-Fe$_2$O$_3$ converted to elemental Fe in the discharge process, the elemental Fe could not reversibly converted to Fe^{3+} in the following charge process, but converted to FeO, and the reversible charge/discharge process were between FeO and Li$_2$O after the initial charge/discharge process. Y. Xie et al [24] had prepared α-Fe$_2$O$_3$ nanorods by hydrothermal method and the following calcined process. The initial discharge capacity were at the range of 900-1200 mAhg^{-1}, whereas with poor cycle performance.

4. Hollow and core-shell structure construction of transition metal oxide materials and their electrochemical performance

The above examples of the transition metal oxides materials with nanostructure all showed large initial specific capacities, but suffered from large capacity loss
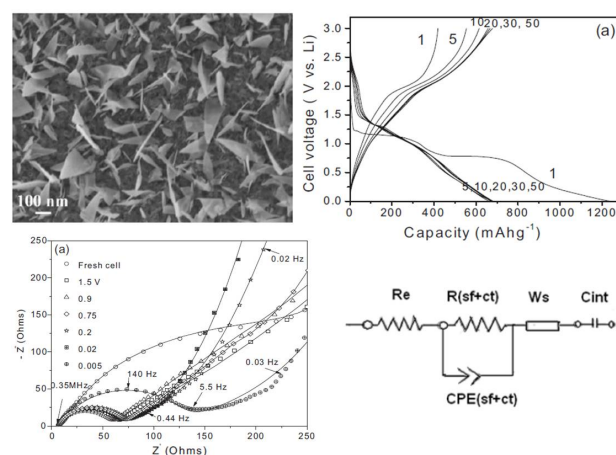

Figure 3 SEM image of α-Fe$_2$O$_3$ nanoflakes grown on a Cu substrate; Galvanostatic charge-discharge curves in the voltage range 0.005-3.0 V (vs. Li) at a current of 65 mAg^{-1}. Nyquist plots (Z′ vs. –Z″) during the first cycle, at various voltages (Discharge cycle) and the fitted data. Reprinted with permission from M.V. Reddy, T. Yu, C.H. Sow, Z.X. Shen, C.T. Lim, G.V. Subba Rao, B.V.R. Chowdari, Adv. Funct. Mater. 2007, 17, 2792–2799 by WILEY publication.

60

Nano Biomed. Eng. 2013, 5(1), 57-64

and poor cycling stability. Enormous mechanical stress and pulverizes occurred during the charge/discharge cycles were usually the reason. The agglomeration of the nano materials was another reason for the poor cycling stability. One effective way to mitigate these problems was to fabricate hollow structured or porous structure. The hollow interior provided extra free space for alleviating the structural strain and accommodating the large volume variation associated with repeated Li^+ insertion/extraction processes, giving rise to improved cycling stability. Forthmore, the porous structure allowed for the easy diffusion of electrolyte into the inner region of the electrode. In this contribution, the hollow and porous structured metal oxides were discussed in this section.

SnO_2 nano materials with hollow spherical morphology were widely researched. T. Hyeon et al [25] had prepared SnO_2 hollow nanosphere by calcination of tin salt/resorcinol-formaldehyde resin. The initial discharge capacity of the hollow SnO_2 nano particles was about 1600 $mAhg^{-1}$, which was 600 $mAhg^{-1}$ higher than the solid SnO_2 nano particles. Although the cycling stability was not very good, the hollow SnO_2 nano particles still had 200 $mAhg^{-1}$ higher than the solid material. The detailed morphology and electrochemical performance were shown in Figure 4.

Pillow-shaped porous hollow CuO was prepared by a template-free method by L.H. Yue et al [26]. First, highly crystallized CuC_2O_4 precursor with micron-size in high dispersivity was prepared through a hydrothermal method. Then, porous hollow CuO was obtained by thermal treatment of the as-prepared precursor. From the second cycle, the discharge capacity persisted on about 400 $mAhg^{-1}$. It exhibited high average coulombic

efficiency (98.3%) and capacity retention (83.3% of the discharge capacity of the second cycle after 50 cycles) at a current rate of 0.1 C, which could be seen in Figure 5.

Apart from spherical hollow nanoparticles, nano materials with specific shapes were also had been reported. For an example, X.W. Lou et al [27] reported a scalable synthesis of Fe_2O_3 microboxes with various shell structures based on simple annealing of pre-formed prussian blue (PB) microcubes. The strategy for synthesizing Fe_2O_3 microboxes was depicted in Figure 6. First, highly uniformed PB microcubes were synthesized. Then, PB microcubes were converted to Fe_2O_3 microboxes by subsequent thermal transformation process. There were three types of Fe_2O_3 microboxes, porous Fe_2O_3 microboxes, and hierarchical Fe_2O_3 microboxes. The Fe_2O_3 microboxes obtained with distinct morphologies and structures were displayed in Figure 6. The initial discharge capacities of the three samples were about 1200-1300 $mAhg^{-1}$. Despite the initial capacity loss of ca. 20%, which was considered quite low for transition metal oxide based anodes, all three samples displayed excellent cycling stability with almost no fading of capacity over the first 30 cycles. In particular, the hierarchical Fe_2O_3 microboxes exhibited the highest reversible capacity of 945 $mAhg^{-1}$ in the 30th cycle. From the second cycle onward, the Fe_2O_3 microboxes exhibited a coulombic efficiency of ~95%.

All the above examples of hollow and porous structured transition metal oxides materials showed large initial specific capacities. Different to the solid nano materials, all the samples displayed excellent cycling stability. Apart from hollow and porous structure construction, shell coating were also an effective strategy to improve the cycling stability. Carbon coating was a widely used
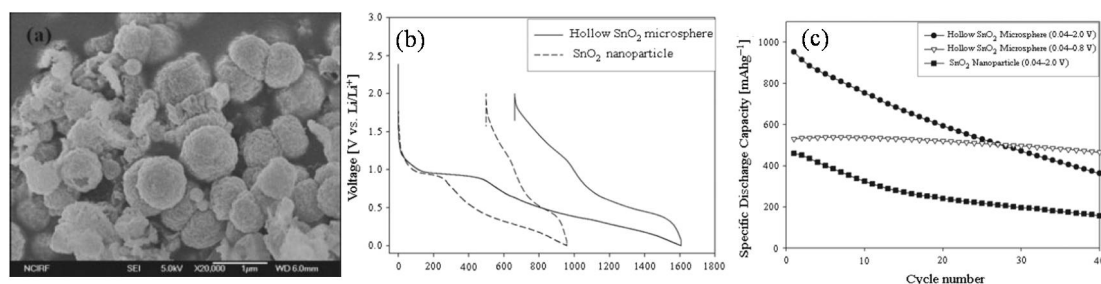

Figure 4 SEM images, the galvanostatic charge-discharge curves in the voltage range 0.04-2.0 V of hollow SnO_2 microspheres, and the cycling profile of hollow SnO_2 microspheres and SnO_2 nanoparticles. Reprinted with permission from S.J. Han, B. Jang, T. Kim, S.M. Oh, T. Hyeon, Adv. Funct. Mater. 2005, 15, 1845-1850 by WILEY publication.
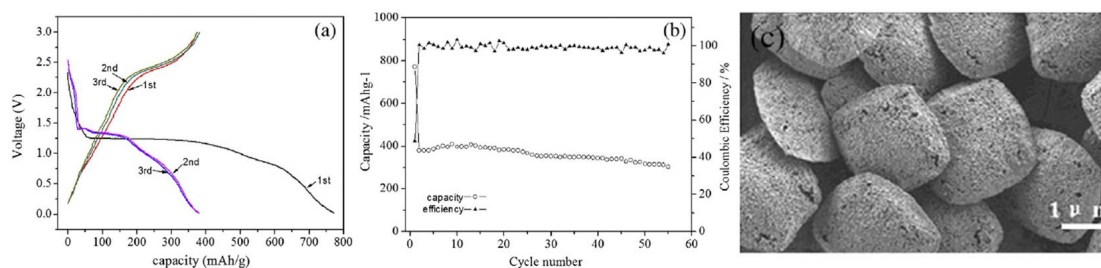

Figure 5 Charge-discharge curves, the cycling behavior and SEM images of the porous pillow-shaped CuO. Reprinted with permission from M. Wan, D.L. Jin, R. Feng, L.M. Si, M.X. Gao, L.H. Yue, Inorg. Chem. Comm. 2011, 14, 38-41 by Elsevier publication.
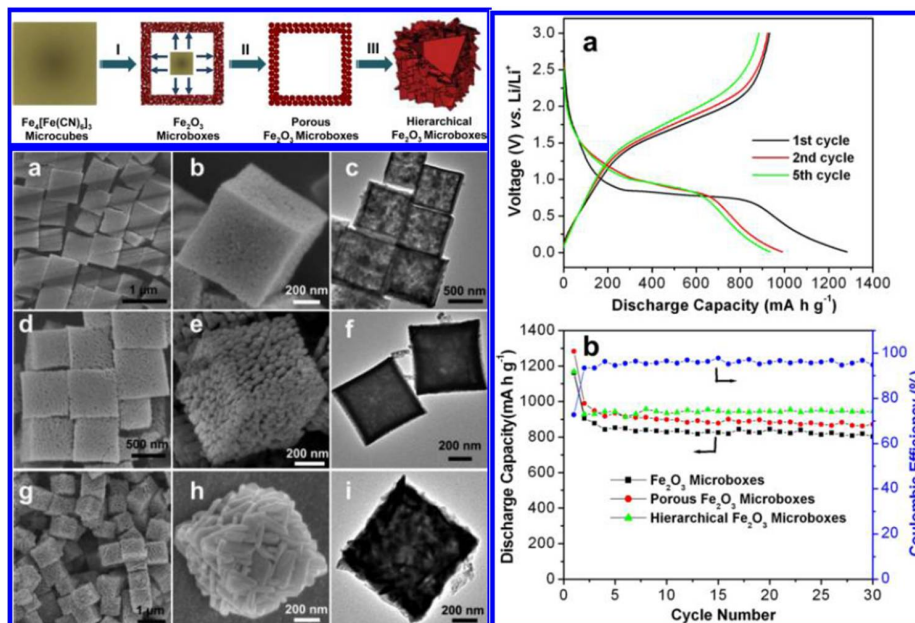
Nano Biomed. Eng. 2013, 5(1), 57-64

61

Figure 6 Schematic illustration of the formation of hollow Fe_2O_3 microboxes and the evolution of the shell structure with the increasing calcination temperature.(a, b, d, e, g, h) FESEM and (c, f, i) TEM images of hollow Fe_2O_3 microboxes obtained at (a, b, c) 350 °C, (d, e, f) 550 °C, and (g, h, i) 650 °C. Discharge-charge voltage profiles of porous Fe_2O_3 microboxes obtained at 550 °C. (b) Cycling performance of Fe_2O_3 microboxes (350 °C), porous Fe_2O_3 microboxes (550 °C), and hierarchical Fe_2O_3 microboxes (650 °C) and Coulombic efficiency of porous Fe_2O_3 microboxes (550 °C) over the voltage range 0.01-3.0 V vs Li/Li$^+$ at the same current density of 200 mA g^{-1}.Reprinted with permission from L. Zhang, H.B. Wu, S. Madhavi, H.H. Hng, X.W. Lou, J. Am. Chem. Soc. 2012, 134, 17388-17391 by ACS publication.

strategy to improve the electrical conductivity of the electrode materials for LIBs. For example, Y.G. Guo and L.J. Wan et al [28] had synthesized monodispersed Fe_3O_4 spindles by a hydrothermal method. Then the as-prepared Fe_3O_4 spindles were mixed with glucose, and the mixture was transferred to a Teflon autoclave, and was heated at 190 °C. The carbonprecursor coated hematite particles were harvested here. Then the sample was calcined in N_2 atmosphere and the carbon coated Fe_3O_4 spindles could be obtained. The Fe_3O_4-C nanospindles showed high reversible capacity (~745mAhg^{-1} at C/5 and ~600 mAhg^{-1} at C/2), high coulombic efficiency in the first cycle, as well as significantly enhanced cycling performance and high rate capability compared with bare hematite

spindles and commercial magnetite particles. As shown in Figure 7, the first specific charge capacity of Fe_3O_4-C composite was as high as 749 mAhg^{-1}, approaching ~93% of its theoretical specific capacity (805 mAhg^{-1}). The capacity of the composite remained unchanged through the subsequent four discharge/charge cycles. When cycles were tested at a relatively high current rate of 0.5C for the subsequent 80 cycles, the capacity of the bare α-Fe_2O_3 and the commercial Fe_3O_4 faded to 250 and 300 mAhg^{-1} immediately and then gradually decreased to 105 and 152 mAhg^{-1}, respectively. The capacity of Fe_3O_4-C composites also decreased to about 600 mAhg^{-1}, but the capacity remained 530 mAhg^{-1} even after another 80 discharge/charge cycles, which is almost 5 times of
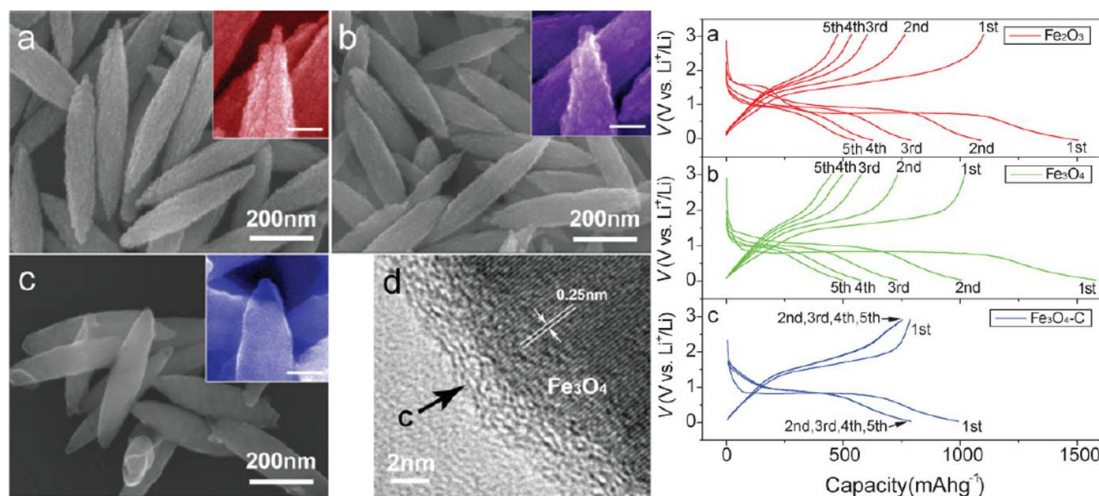

Figure 7 (a) SEM image of the as-synthesized hematite spindles. (b) SEM image of the carbon precursor coated hematite spindles. (c) SEM image of the carbon coated Fe_3O_4 spindles (Fe_3O_4-C composites). (d) high-resolution TEM image of the Fe_3O_4-C composites. The insets are close views of corresponding samples, all unmarked scale bars are 50 nm. And the discharge/charge profiles of (a) bare hematite spindles, (b) commercial magnetite particles, and (c) Fe_3O_4-C composites, at a current rate of C/5. Reprinted with permission from W.M. Zhang, X.L. Wu, J.S. Hu, Y.G. Guo, L.J. Wan, Adv. Funct. Mater. 2008, 18, 3941-3946 by WILEY publication.

62

Nano Biomed. Eng. 2013, 5(1), 57-64

that of the bare α-Fe$_2$O$_3$ spindles and 3.5 times of that of the commercial Fe$_3$O$_4$ particles. The improvements could be attributed to the uniform and continuous carbon coating layers, which have several functions, including: (1) maintaining the integrity of particles, (2) increasing the electronic conductivity of electrodes leading to the formation of uniform and thin solid electrolyte interphase (SEI) films on the surface, and (3) stabilizing the as-formed SEI films. The results gave clear evidences of the utility of carbon coatings to improve the electrochemical performance of nanostructured transition metal oxides as superior anode materials for LIBs.

Apart from the the Fe$_3$O$_4$-C composite, SnO$_2$@carbon, CuO@carbon, oxides@ carbon composites were all prepared. The capacity of CuO@carbon composite was about 500 mAhg^{-1} after 50 cycles. The capacity of SnO$_2$@carbon composite was about 500 mAhg^{-1} after 100 cycles. They all indicated enhanced cycling performance. Y.D. Li et al [29] addressed a general and facile one-pot hydrothermal method was developed to prepare oxide@C core-shell nanostructures with carbonaceous polysaccharide shells and oxides (including hydroxides or complex oxides) cores. The electrochemical characterization on calcined SnO$_2$@C nanostructures showed good cycling performance.

Graphene, as a new component of carbon materials, had also been used as coating shell in the LIBs anode materials. Y. Cui and H.J. Dai et al [30] developed two-step solution-phase reactions to form hybrid materials of Mn$_3$O$_4$ nanoparticles on reduced graphene oxide (RGO) sheets for lithium ion battery applications. The Mn$_3$O$_4$ nanoparticles formed on RGO showed a high specific capacity up to ~900 mAhg^{-1}, near their theoretical capacity, with good rate capability and cycling stability, owing to the intimate interactions between the graphene substrates and the Mn$_3$O$_4$ nanoparticles grown atop. For the free Mn$_3$O$_4$ nanoparticles, the capacity was about 200 mAhg^{-1}. The graphene hybridized composite showed 700 mAhg^{-1} higher in capability. So the Mn$_3$O$_4$/RGO hybrid could be a promising candidate material for a high-capacity, low-cost, and environmentally friendly anode for lithium ion batteries. Y.G. Guo et al [31] had developed SnO$_2$/RGO hybrid, which had specific charge capacity of the composite was 786 mAhg^{-1} in the first cycle and 558 mAhg^{-1} after 50 cycles. The cycling performance had been drastically improved. For the free SnO$_2$ powder, the initial specific capacity was 838 mAhg^{-1}. After 50 cycles, the capacity decreased dramatically to 137 mAhg^{-1}, showing only 18% retention of its initial capacity. X.L. Feng et al [32] presented a two-dimensional (2D) core-shell nanostructure constructed by confining the well-defined graphene based metal oxides nanosheets (G@MO) within carbon layers. The sample had both the advantages of graphene and could tackle the deformation of MO nanoparticles while keeping the overall electrode highly conductive and active in lithium storage. The G@SnO$_2$@C sample had the capacity of 800 mAhg^{-1} at the rate of 200 mAg^{-1} after 100 cycles. The as-prepared G@

Fe$_3$O$_4$@C sample had the capacity of 920 mAhg^{-1} at the rate of 200 mAg^{-1} after 100 cycles.

In summary, there are more and more researches on the transition metal oxides as LIBs anode materials. They usually focus on preparing transition metal oxides into nanometer scale with variaties of morphologies and the hollow and core-shell structures to improve their electrochemical performance. Although many studies have done on transition metal oxides as LIBs anode materials, this region even needs more powerful research. For examples, the issues now are how to transform these scientific results to practical application, and how to transform the laboratory synthesis to large scale industrial production.

5. Conclusions

Transition metal oxides are promising anode materials for Li-ion batteries due to their high theoretical capacity (> 600 mAhg^{-1}), good rate capability, good safety, environmental friendliness and relatively low cost. But the disadvantage of this kind of materials is the poor cycling performance. To make materials into nanometer scale and hollow, core-shell structure could improve the cycling performance. Now most efforts have made on their hybrid materials preparation. But this region even needs more powerful research. For examples, the issues now are how to transform these scientific results to practical application, and how to transform the laboratory synthesis to large scale industrial production. We have long way to go in this research area to achieve the valuable application as soon as possible.

References

1 Tarascon J. M., Armand M., Issues and challenges facing rechargeable lithium batteries. *Nature* 2001, 414 (6861), 359-367.
2 Wu Y., Wan, C., Jiang c., Lithium-ion secondary battery. *Chemical Industry Press* 2002.
3 Wu Y., Dai X., Ma J., Cheng Y. Lithium-ion battery-Applications and Practice. *Chemical Industry Press* 2004.
4 Reeves S. D., Morris R. S. Improved MCMB anodes by surface modification with self-assembling nonionic surfactants. *Electrochem. Solid St. Chem.* 2004, 7 (8), B29-B30.
5 Mochida I., Ku C. H., Korai Y. Anodic performance and insertion mechanism of hard carbon prepared from synthetic isotropic pitches. *Carbon* 2001, 39 (3), 399-410.
6 EunJoo Y., Kim J., Hosono E., Hao-shen Z., Kudo T., Honma I. Large reversible Li storage of graphene nanosheet families for use in rechargeable lithium ion batteries. *Nano Lett.* 2008, 8 (8), 2277.
7 Wang F., Zhao, M.; Song, X., Nano-sized SnSbCux alloy anodes prepared by co-precipitation for Li-ion batteries. *J. Power Sources* 2008, 175 (1), 558-563.
8 Yu Y., Chen, C.H., Shi, Y. A tin-based amorphous oxide composite with a porous, spherical, multideck-cage morphology

Nano Biomed. Eng. 2013, 5(1), 57-64

HOST 63

as a highly reversible anode material for lithium-ion batteries. *Adv. Mater.* 2007, 19 (7), 993-998

9 Min Gyu, K.; Jaephil, C., Nanocomposite of amorphous Ge and Sn nanoparticles as an anode material for Li secondary battery. *J. Electrochem. Soc.* 2009, 156 (4), A277-82.

10 Hu Y.S., Demir-Cakan R., Titirici M.-M., Mueller J. O., Schloegl R., Antonietti M., Maier J. Superior storage performance of a $Si@SiOx/C$ nanocomposite as anode material for lithium-ion batteries. *Angew. Chem. Int. Ed.* 2008, 47 (9), 1645-1649.

11 Cui L.F., Ruffo R., Chan C.K., Peng H., Cui Y. Crystalline-amorphous core-shell silicon nanowires for high capacity and high current battery electrodes. *Nano Lett.* 2009, 9 (1), 491-495.

12 Poizot P., Laruelle S., Grugeon S., Dupont L., Tarascon J.M. Nano-sized transition-metaloxides as negative-electrode materials for lithium-ion batteries. *Nature* 2000, 407 (6803), 496-499.

13 Wang P.C., Ding H.P., Bark T., Chen C.H. Nanosized alpha-Fe_2O_3 and Li-Fe composite oxide electrodes for lithium-ion batteries. *Electrochim. Acta* 2007, 52 (24), 6650-6655.

14 Zhang D.W., Yi T.H., Chen C.H. Cu nanoparticles derived from CuO electrodes in lithium cells. *Nanotechnology* 2005,16 (10),2338-2341

15 Chen J., Xu L.N., Li W.Y., Gou X.L. alpha-Fe_2O_3 nanotubes in gas sensor and lithium-ion battery applications. *Adv. Mater.* 2005, 17 (5), 582-587.

16 Zhao Q., Xie Y., Dong T., Zhang Z. Oxidation-crystallization process of colloids: An effective approach for the morphology controllable synthesis of SnO_2 hollow spheres and rod bundles. *J. Phys. Chem. C* 2007, 111 (31), 11598-11603.

17 Yingying H., Xintang H., Kai W., Jinping L., Jian J., Ruimin D., Xiaoxu J., Xin L. Kirkendall-effect-based growth of dendrite-shaped CuO hollow micro/nanostructures for lithium-ion battery anodes. *J. Solid St. Chem.* 183 (3), 662-7.

18 Park M.S., Wang G.X., Kang Y.M., Wexler D., Dou S.X., Liu H.K., Preparation and electrochemical properties of SnO_2 nanowires for application in lithium-ion batteries. *Angew. Chem. Int. Ed.* 2007, 46 (5), 750-753.

19 Wang C., Zhou Y., Ge M., Xu X., Zhang Z., Jiang J.Z. Large-scale synthesis of SnO_2 nanosheets with high Lithium storage capacity. *J. Am. Chem. Soc.* 132 (1), 46-49.

20 Xiang J.Y., Tu J.P., Zhang L., Zhou Y., Wang X.L., Shi S.J. Self-assembled synthesis of hierarchical nanostructured CuO with various morphologies and their application as anodes for lithium ion batteries. *J. Power Sources* 195 (1), 313-319.

21 Grugeon S., Laruelle S., Herrera-Urbina R., Dupont L., Poizot P., Tarascon J.M. Particle size effects on the electrochemical performance of copper oxides toward lithium. *J. Electrochem. Soc.* 2001, 148 (4), A285-A292.

22 Debart A., Dupont L., Poizot P., Leriche J.B., Tarascon J.M. A transmission electron microscopy study of the reactivity mechanism of tailor-made CuO particles toward lithium. *J. Electrochem. Soc.* 2001, 148 (11), A1266-A1274.

23 Reddy M.V., Yu T., Sow C.H., Shen Z.X., Lim C.T., Rao G.V.S., Chowdari B.V.R. alpha-Fe_2O_3 nanoflakes as an anode material for Li-ion batteries. *Adv. Funct. Mater.* 2007, 17 (15), 2792-2799.

24 Wu C., Yin P., Zhu X., OuYang C., Xie Y. Synthesis of hematite (alpha-Fe_2O_3) nanorods: Diameter-size and shape effects on their applications in magnetism, lithium ion battery, and gas sensors. *J. Phys. Chem. B* 2006, 110 (36), 17806-17812.

25 Sangjin H., Byungchul J., Taeahn K., Oh S. M.,Taeghwan H. Simple synthesis of hollow tin dioxide microspheres and their application to lithium-ion battery anodes. *Adv. Funct. Mater.* 2005, 15 (11), 1845-50.

26 Mei W., Dalai J., Ran F., Limin S., Mingxia G., Linhai Y. Pillow-shaped porous CuO as anode material for lithium-ion batteries. *Inorg. Chem. Commun.* 14 (1), 38-41.

27 Zhang L., Wu H.B., Madhavi S., Hng H.H., Lou X.W. Formation of Fe_2O_3 microboxes with hierarchical shell structures from metal-Organic frameworks and their Lithium storage property. *J. Am. Chem. Soc.* 134 (42), 17388-17391.

28 Zhang W.M., Wu X.L., Hu J.S., Guo Y.G., Wan L.J. Carbon Coated Fe_3O_4 nanospindles as a superior anode material for Lithium-Ion batteries. *Adv. Funct. Mater.* 2008, 18 (24), 3941-3946.

29 Sun X., Liu J., Li Y. Oxides@C core-shell nanostructures: One-pot synthesis, rational conversion, and Li storage property. *Chem. Mater.* 2006, 18 (15), 3486-3494.

30 Wang H., Cui L.F., Yang Y., Casalongue H.S., Robinson J. T., Liang Y., Cui Y., Dai H. Mn_3O_4-graphene hybrid as a high-capacity anode naterial for Lithium-ion batteries. *J. Am. Chem. Soc.* 132 (40), 13978-13980.

31 Zhang L.S., Jiang L.Y., Yan H.J., Wang W.D., Wang W., Song W.G., Guo Y.G., Wan L.J. Mono dispersed SnO_2 nanoparticles on both sides of single layer graphene sheets as anode materials in Li-ion batteries. *J. Mater. Chem.* 20 (26), 5462-5467.

32 Su Y., Li S., Wu D., Zhang F., Liang H., Gao P., Cheng C., Feng X. Two-dimensional carbon-coated graphene/metal oxide hybrids for enhanced Lithium storage. *Acs Nano* 6 (9), 8349-8356.

64

Nano Biomed. Eng. 2013, 5(1), 57-64